Enabling the Smart and Flexible Management of Energy Prosumers via the Energy Router With Parallel Operation Mode

YINGSHU LIU, XI CHEN, YAO WU, KE YANG, JIEBEI ZHU, AND BIN LI

School of Electrical and Information Engineering, Tianjin University, Tianjin 300072, China

Corresponding author: Yingshu Liu (liu_ysh@tju.edu.cn)

ABSTRACT With the increasing penetration of renewable distributed generations (DGs), large numbers of "energy prosumers" are emerging rapidly. There will be severe impacts on the utility grid if these renewable DGs are not managed properly. Smart electrical power devices which enable high flexibility in energy management, alleviation in harmonic pollutions and friendly interactions with the utility grid are needed urgently. To meet all these requirements, a novel energy router which enables a unique parallel operation mode to the energy prosumer is presented. Facilitated with a bi-directional DC/AC converter, a switch array module and a fuzzy logic based hierarchical control strategy, the presented energy router enables plug-and-play connections and reliable energy management for the energy prosumer. The switch array and the parallel mode enable the loads to be flexibly scheduled to reduce energy cost and improve system performance. MATLAB/Simulink model of the energy prosumer is set up and a fuzzy logic based hierarchical control strategy is implemented for transient power balance control in various operation modes. Simulation results have demonstrated high flexibility, stability and feasibility of the proposed energy router in energy management of the prosumer, which will contribute to the better utilization of the ever-growing renewable energies.

I. INTRODUCTION

Driven by the ever-growing energy consumption demand and the concern for environment protection, the existing electrical power grid will be shifting from the traditional single sourced, radial network to the multi-sourced, meshed, and renewable energy based power system of the next generation – the Energy Internet [1], [2]. Both Europe and the United States have put forward their plans for 100% renewable energy supply by 2050 [3], [4]. According to the US plan, utility-scale solar stations and rooftop photovoltaic (PV) systems shall account for 37.9% of the total renewable energies, while rooftop PV generations shall occupy 19% of the entire solar generations.

With the increasing penetration of distributed renewable generations, residential or commercial energy consumers with distributed renewable generations like rooftop PVs or wind turbines are emerging rapidly. These entities, playing the roles of both energy consumers and producers, are referred to as "energy prosumers" [5], [6]. This new energy paradigm will have remarkable effects on the power system due to the following reasons: 1) with their excess energy productions, prosumers will have comprehensive interactions with the utility grid. It is both an opportunity and a challenge to the power utility and the users as well. Existing patterns of energy consumption and demand side management need to be improved. 2) On the other hand, various impacts will be expected as large numbers of renewable generations are connected to the utility grid. The intermittent and unpredictable nature of the renewable energies will inevitably cause fluctuations in power, frequency, and line voltage. During high generation and low load periods, there is even possibility of reverse power flow in the low voltage (LV) feeder [7], [8]. These factors may cause severe problems from power quality and energy efficiency at the user side to instability at the level of distribution network.

The associate editor coordinating the review of this manuscript and approving it for publication was Seyyed Ali Pourmousavi Kani.

Many works have been carried out to tackle the above mentioned problems during the last decade. One of the most promising technologies among them is the energy router (also known as the electrical power router). Facilitated with distributed energy source integration, flexible power flow management and wide area information interaction, the energy router has demonstrated great potential in the future Energy Internet. Solid state transformer, which is the core of medium voltage (MV) energy router, has been developed for voltage step-down and power flow management at the grid level [1], [9]–[11]. With high voltage (HV) energy routers, the power system can even be divided into smaller segmented asynchronous sub-grids, which will be able to accommodate high penetrations of renewable energies, prevent cascading outages and even provide identifiable tagged electricity deliveries [2]. A hierarchical optimization strategy is put forward for the energy router to reduce the complexity of centralized optimal dispatch on large-scale systems and protect the information privacy of different sub-grids in [12]. At the microgrid level, energy router manages the power flow among microgrids to enable proper energy share, avoid congestions and mitigate unbalanced 3 phase AC loading [13]–[15]. A peer to peer control strategy is proposed for this energy router to achieve distributed power sharing in both grid-connected and islanded mode in [16]. For residential users, energy router will serve as an intelligent and multi-functional energy interface between the home area energy network and the power grid [17]. LV power flow can be managed through a direct "circuit switching" mechanism [18], or be transferred in "discrete energy packets" with tag information on energy source and destination [19].

At residential level, there will also be severe impacts on the distribution network if large numbers of distributed renewable sources are not managed properly. Smart devices which enable high flexibility in energy management, alleviation in harmonic pollutions and friendly interactions with the utility grid are needed badly. However, there is still lack of practical and reliable solutions to meet all these requirements. To address this problem, we develop a novel energy router which enables a unique "parallel operation mode" to the energy prosumer.

The remainder of the paper is organized as follows: In Section II, the schematic of the energy router which enables the parallel operation mode is described and its working mechanism is analyzed in detail. The fuzzy logic based hierarchical control strategy for the energy prosumer is presented in Section III. Simulation model is set up in Section IV, and cases study are presented to demonstrate the performances of the prosumer in multiple operation modes enabled by the energy router. Finally, Section V concludes this paper and proposes the plan for future work.

II. ENERGY ROUTER & PARALLEL OPERATION MODE
A. SCHEMATIC OF THE ENERGY ROUTER
An energy prosumer is typically composed of renewable generations, energy storage (ES) units and various types of loads,
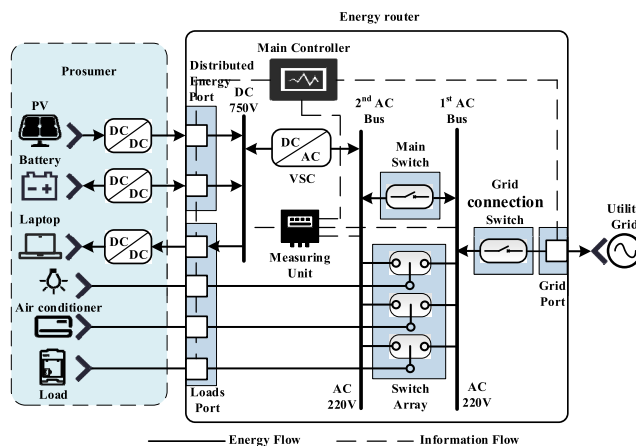

FIGURE 1. Hardware schematic of the energy router for prosumers.

which are all integrated through the energy router, as depicted in Fig.1. The energy router itself is a hybrid AC/DC microgrid, which has two AC buses, one DC bus, a bidirectional Voltage Source Converter, (hereinafter referred to as the main converter or VSC) which connects the DC bus and one of the AC bus (hereinafter referred to as 2nd AC bus), power source ports, load ports, a "main switch" and an array of single-pole double-throw (SPDT) switches between the two AC buses.

A PV unit, as the renewable generation considered in this paper, connects to the DC bus through a DC/DC converter with maximum power point tracking (MPPT) module. A battery unit connects to the DC bus through a DC/DC converter, thus makes DC bus the "energy pool" or "energy buffer" of the whole system.

The utility grid is connected to another AC bus (hereinafter referred to as 1st AC bus). The "main switch" between the 1st and 2nd AC buses is used to put the energy router in grid connected mode, while the array of SPDT switches enable the loads to be connected to different AC buses according to specified energy management strategies.

B. PARALLEL OPERATION MODE FACILITATED BY THE ENERGY ROUTER
Facilitated with the SPDT switch array between the two AC power lines, the energy router will be in a unique operating status when the main switch is open, the grid connection switch is closed and the loads are connected to different power lines. In this situation the energy prosumer is in neither grid connected nor islanded operation mode, since the loads connected to the 1st AC bus are powered by the utility grid, while the rest of the loads are powered through the islanded 2nd AC bus. We define this unique status as the "parallel operation mode".

The transitions among the three operation modes are demonstrated in Fig. 2, which can be summarized as:

1) Grid connected mode to the islanded mode – the grid connection switch is turned from closed to open, and the energy prosumer will transfer from the grid connected mode to the islanded mode.
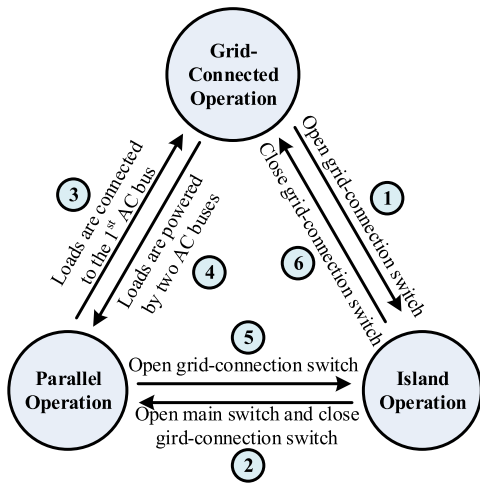
2) Islanded mode to grid connected mode – when the grid connection switch is turned on, the energy prosumer will transfer from the islanded mode to the grid connected mode.

3) Parallel operation mode to grid connected mode – when all loads are connected to the 1st AC bus because of no distributed generation (DG) power output, the prosumer will transfer from parallel operation mode to grid connected mode.

4) Grid connected operation mode to parallel mode – when DG power increases and loads are powered by two AC buses, the prosumer will transfer from grid connected mode to parallel operation mode.

5) Parallel operation mode to islanded mode – when the grid connection switch is switched off, the prosumer will transfer from parallel operation mode to islanded mode.

6) Islanded operation mode to parallel mode – when the grid-connection switch is switched on and the main switch is switched off, the prosumer will transfer from islanded mode to parallel operation mode.

C. DISTINGUISHING FEATURES OF THE PARALLEL OPERATION MODE

The presented energy router with parallel operation mode enhances reliability and flexibility to the prosumer due to the following distinguishing features:

1) HIGHER FLEXIBILITY IN ENERGY MANAGEMENT

Smart energy management can be achieved with proper uses of the switch array. For example, appliances are scheduled to the appropriate bus in order to ''match'' with power sources according to their requirement on power quality or other energy management strategies.

2) ALLEVIATION OF THE HARMONIC POLLUTIONS TO THE UTILITY GRID

In parallel operation mode, the 2nd AC bus is isolated from the utility grid, thus avoids harmonic pollutions caused by the
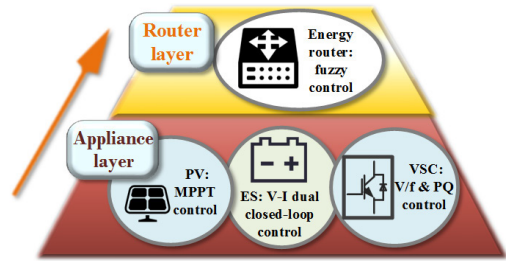

FIGURE 3. Brief sketch of the hierarchical control strategy.

main converter and fluctuations of the renewable generations. Appliances not sensitive to harmonics, such as heater and devices with AC/DC adapters (LED lamps, chargers, et al), can be preferentially switched to the 2nd AC bus, while those with stringent energy quality requirements are switched to the 1st AC bus.

3) MORE FRIENDLY INTERACTION WITH THE UTILITY GRID

With the abovementioned flexibilities enabled by the parallel operation mode, energy interaction between the prosumer and utility grid can be improved, which helps to reduce the impact of renewable energy fluctuations on distribution network.

Proper use of the switch array enables much flexibility in peak load curtailment and demand side management. Enhanced protection to the utility grid in case of fault in the prosumer can be achieved within the parallel mode, since the two AC power lines are supplying power separately. Even the problem of three-phase load unbalances can be alleviated through single-phase energy management using the switch array.

4) ENHANCED INTERCONNECTIONS OF ENERGY PROSUMERS

Due to the intermittent and unpredictable nature of the renewable energies and relatively small scales of the energy prosumers, it is preferable that neighboring prosumers should work as a group to improve their operational performances and alleviate the effect of power impacts to the utility grid [20]–[23].

Under the parallel operation mode, it is very convenient for prosumers to operate in clusters, then the impact caused by renewable generation fluctuations and harmonic components of the power electronics devices to the grid can be alleviated remarkably. Direct energy exchanges within the interconnected prosumer cluster are also available and easy if they are all connected through their common 2nd AC buses.

III. HIERARCHICAL CONTROL STRATEGY

The brief sketch of the hierarchical control strategy is depicted in Fig. 3. The strategy is composed of two layers: the appliance layer control and the router layer control.

The appliance layer is responsible for the control of DGs, energy storage unit and appliances, including MPPT control for PV, voltage current dual closed-loop control for ES unit
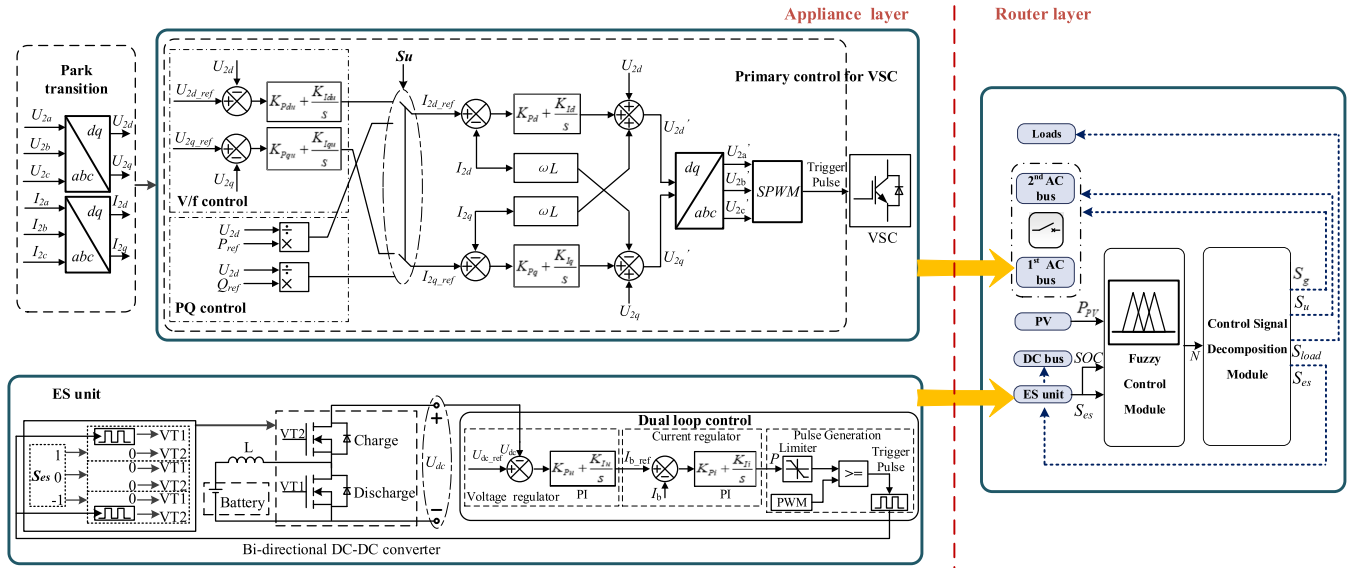
FIGURE 4. Main body of the schematic diagram of the hierarchical control strategy.

to stabilize voltage of the DC bus, and V/f or PQ control for VSC to stabilize voltage of the AC power line. Router layer control is implemented at the energy management level of the prosumer, which is a fuzzy logic control (FLC) based coordinated operation of the main converter, the ES unit, DGs and the switch array, aiming for maintaining power balance, improving the efficiency of DG utilization and management of operation mode transformation of the energy prosumer. The main body of the schematic diagram of the hierarchical control strategy for the energy prosumer system, including the controller schematics of the VSC, the ES unit, the fuzzy control module along with the interactions between them, is depicted in Fig. 4.

A. APPLIANCE LAYER CONTROL

The islanding mode of V/f control strategy for VSC is included in Fig. 4. The output of this control strategy is used to generate trigger pulses for VSC. With this control, the 2nd AC bus voltage amplitude and frequency are maintained at expected values.

Under dq-axis synchronous reference frame, the d-axis voltage vector U_{2d}, representing appliance voltage magnitude, is controlled at constant values U_0 (e.g. 1 pu), whereas q-axis voltage vector U_{2q}, representing any appliance voltage phase angle change, is regulated at 0 so that the appliance frequency remains constant.

$$\begin{cases} U_{2d\_ref} = U_0 \\ U_{2q\_ref} = 0 \end{cases} \quad (1)$$

where U_{2d_ref} and U_{2q_ref} are d- and q-axis reference voltage at the inverter's Point of Common Coupling (PCC), and U_0 is the voltage magnitude (In this paper $U_0 = 380V$).

To regulate the voltage at PPC, the grid connected mode is adopted. The dynamic equations of the VSC in q-axis synchronous reference frame are:

$$\begin{cases} U'_{2d} = U_{2d} + \omega L I_{2q} + L \dfrac{dI_{2d}}{dt} \\ U'_{2q} = U_{2q} - \omega L I_{2d} + L \dfrac{dI_{2q}}{dt} \end{cases} \quad (2)$$

where L is the total inductance between the VSC and the PCC; U'_2 and U_2 are the voltages at the VSC terminals and PCC, respectively.

To track the reference currents I_{2d_ref} and I_{2q_ref}, the inner current control uses proportional–integral (PI) controllers with feedback to regulate the current vectors I_{2d} and I_{2q} as shown in Fig. 4. Therefore, the VSC voltage vector references U'_{2d} and U'_{2q} for the VSC are computed as follows:

$$\begin{cases} U'_{2d} = U_{2d} + \omega L I_{2q} + \left(k_{pd} + \dfrac{k_{id}}{s}\right)\left(I_{2d\_ref} - I_{2d}\right) \\ U'_{2q} = U_{2q} - \omega L I_{2d} + \left(k_{pq} + \dfrac{k_{iq}}{s}\right)\left(I_{2q\_ref} - I_{2q}\right) \end{cases} \quad (3)$$

The control strategy for ES unit is included in Fig. 5. Voltage current cascaded closed-loop is used to control the triggering pulses of VT1 and VT2. The DC bus voltage difference between reference and actual measured value is processed by a PI controller to calculate the reference current of the battery. The governing equation of voltage loop is given as:

$$I_{b\_ref} = \left(K_{Pu} + \dfrac{K_{Iu}}{s}\right)\left(U_{dc\_ref} - U_{dc}\right) \quad (4)$$

The battery current difference between reference and measured value is sent to PI controller. Governing equation of current loop to compute the desired battery voltage magnitude reference P is given as:

$$P = \left(K_{Pi} + \dfrac{K_{Ii}}{s}\right)\left(I_{b\_ref} - I_b\right) \quad (5)$$
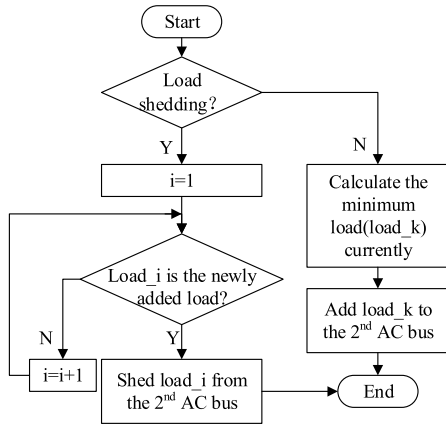
FIGURE 5. Flowchart of load matching process.

Through PI controller, the battery voltage magnitude reference P is sent to PWM module so as to generate triggering pulses for the MOSFET. Before cascaded closed-loop is implemented in this ES unit, charge-discharge switch control signal S_{es} should be considered. $S_{es} = 1$ controls the ES unit to discharge with VT1 turned on and VT2 turned off. Triggering pulse of VT1 is generated by cascaded closed-loop control. $S_{es} = 0$ operates ES unit to stop working with VT1 and VT2 both turned off. $S_{es} = -1$ controls ES unit to charge with VT1 turned off and VT2 turned on. Triggering pulse of VT2 is generated by cascaded closed-loop control.

B. ROUTER LAYER CONTROL

The top level control for the prosumer is designed for two purposes: 1) ensure full utilization of all the DGs. 2) maintain the DC and AC bus voltage stabilization for power balance while the main converter is in operation.

The first problem can be formulated as:

$$Max \ Uti(P_{pv}) \tag{6}$$

which is subjected to the constraints derived from the second problem:

$$SOC^{min} \le SOC \le SOC^{max} \tag{7}$$

$$\left| U_{dc} - U_{dc}^{ref} \right| \le 5\% U_{dc}^{ref} \tag{8}$$

$$|U_2 - U_1| \le 10\% U_1 \tag{9}$$

$$|f_2 - f_1| \le 0.5Hz \tag{10}$$

where $Uti(P_{PV})$ means the utilization of PV. SOC^{min} and SOC^{max} are the minimum and maximum of State of Charge (SOC) of ES unit. U_1, U_2 and f_1, f_2 are the voltage and frequency amplitudes of two AC buses. In the parallel operation mode, loads are powered by two AC buses, so

$$P_{l\_bus1} + P_{l\_bus2} = P_{load} \tag{11}$$

$$P_{load} = \sum_{i=1}^{n} p_{l\_i} \tag{12}$$

TABLE 1. Quantitative results of inputs and output.

	Basic Domain	Fuzzy Domain	QF[a]	Fuzzy Subset
P_{pv}	[0, 12kW]	[0, 0.05, 0.55, 1.5]	1/6000	[Z, S, M, B]
SOC	[0, 100]	[0, 0.625, 0.9]	1	[Z, S, B]
S_{es}	[-1, 1]	[-1, 0, 1]	1	[N, Z, P]
N	[-3, 3]	[-3, -2, -1, 0, 1, 2, 3]	1	[NB, NM, NS, ZE, PS, PM, PB]

QF[a] stands for Quantization Factor.

where P_{l_bus1} is the power of the 1st AC bus. P_{l_bus2} is the power of the 2nd AC bus. P_{load} is the power of all the loads. P_{l_i} is the ith load power.

When the ES unit is not fully charged or discharged, its power and charge-discharge control signal can be derived from

$$P_{ES} = P_{pv} - P_{l\_bus2} \tag{13}$$

$$S_{es} = \begin{cases} 1, & P_{ES} < 0 \\ 0, & P_{ES} = 0 \\ -1, & P_{ES} > 0 \end{cases} \tag{14}$$

When the ES unit is fully charged and $P_{pv} > P_{l\_bus2}$, the surplus power will be absorbed by utility grid, which is

$$P_{grid} = P_{pv} - P_{l\_bus2} \tag{15}$$

where P_{grid} is the power absorbed by utility grid from the energy prosumer.

C. FUZZY CONTROL STRATEGY

As illustrated in Fig. 4, the fuzzy controller has three inputs: 1) P_{pv}, which is the PV unit generation. 2) SOC, which indicates the state of charge of the ES unit. 3) S_{es}, which is the operational status (charge/discharge) of the ES unit. The fuzzy control output N is mapped into 4 variables: S_{load}, S_g, S_{es}, S_u which are control signals of the switch array and main switch, ES unit control signal and VSC control signal.

Load matching starts with the load with minimum power P_{lmin}, and next minor power loads, taking "first access, last removal" and "last access, fist removal" as the principle, in order to minimize the switch array action times. After load matching, surplus PV power can be used to charge the ES. As a result, full utilization of DG power utilization can be achieved. Its flowchart is shown in Fig 5.

As for the ES unit, if SOC is less than 90%, it begins to charge until SOC reaches 90%. If SOC is higher than 90%, ES unit begins to discharge until SOC reaches below 35%.

Table 1 shows the quantization of the inputs and output of the fuzzy controller. Domains of the inputs and output vary according to design requirements. The maximum PV output is 12kW. Four variables, namely Z (zero), S (small), M (middle) and B (big), are considered for P_{pv}. Three variables, Z (zero), S (small) and B (big), are considered for SOC. Three variables, N (negative), Z (zero) and P (positive), are considered for S_{es}. Seven variables,
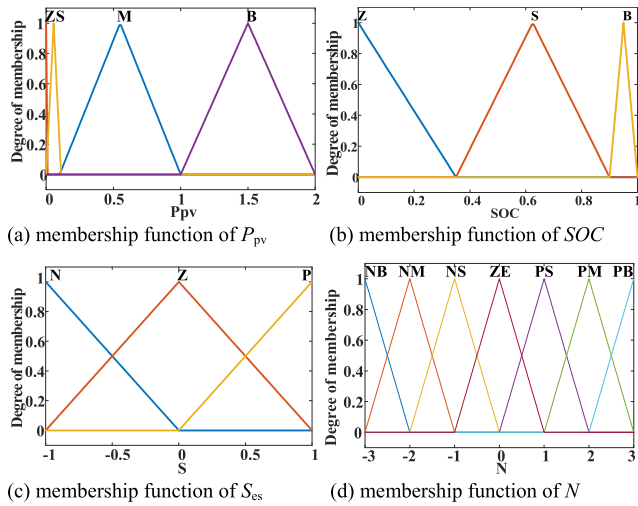
(a) membership function of P_{pv}

(b) membership function of SOC

(c) membership function of S_{es}

(d) membership function of N

FIGURE 6. Triangular membership functions.

TABLE 2. Meanings of the switch signals.

Control Signal	Value	Meaning
S_{load}	0	All loads are connected to the 1st AC bus
	1	All loads are connected to the 2nd AC bus
	-1	Load matching
S_g	0	Main switch is open
	1	Main switch is closed
S_u	0	PQ control is selected for VSC
	1	V/f control is selected for VSC
S_{es}	-1	ES unit charges
	0	ES unit doesn't work
	1	ES unit discharges

NB (negative big), NM (negative middle), NS (negative small), ZE (zero), PS (positive small), PM (positive middle) and PB (positive big), are considered for control output N. The triangular membership functions of inputs and output are established based on the quantization, as depicted in Fig. 6.

The centroid method in (16) is used for defuzzification to get the system operation mode selection signal N.

$$N_{avr} = \frac{\sum_{i=1}^{n} x_i \mu_N(x_i)}{\sum_{i=1}^{n} \mu_N(x_i)} \quad (16)$$

where n $= 4 \times 3 \times 3 = 36$ is the number of fuzzy rules, x_i is the element in N's domain and $\mu_N(x_i)$ is its membership value.

N_{avr} obtained from (16) is not an integer, it needs rounding operation which is conducted with the MATLAB function:

$$N = round(N_{avr}) \quad (17)$$

The fuzzy control output N is designed to make the prosumer operate in one of seven working conditions. Take N as the input of control signal decomposition module, its outputs are mapped into four control signals: S_{load}, S_g, S_u, and S_{es}. Meanings of the signals are indicated in Table 2.

TABLE 3. Fuzzy output vs. control signals.

N	S_{load}	S_g	S_u	S_{es}	Operation Mode
-3	0	0	1	0	Grid connected
-2	-1	0	1	1	Grid connected
-1	0	0	1	-1	Grid connected
0	-1	0	1	-1	Parallel
1	-1	0	1	1	Parallel
2	1	0	1	-1	Islanded
3	1	1	0	0	Islanded

TABLE 4. Simulation parameters.

Parameter	Quantity
Rated power of PV	12kW
Voltage reference of DC bus voltage	750V
Valid value of AC bus rated line voltage	380V
Rated frequency of the 1st AC bus	50Hz
Rated capacity of battery	100Ah
Nominal voltage of battery	12V

The correspondence of fuzzy output N with the control signals are illustrated in Table 3. Assuming the grid connection switch is always closed, then the prosumer's operation modes are: 1) While $N = -3, -2, -1$, the prosumer is in grid-connection mode; 2) While $N = 0, 1$, the prosumer is in parallel mode, considering that PV generation varies constantly, so ES should always be working; 3) While $N = 2, 3$, the prosumer is in islanded mode, assuming that ES does not provide power supply in this mode.

Special precautions are also made to prevent frequent operations of load switching or operation mode switching in short time range, in case DG generations might fluctuate around the level of total load demand. Rules for restrictions on frequent switching within given time range are set: 1) If the prosumer's operation mode is switched more than 5 times within the time range threshold, the prosumer will be mandatorily kept in grid-connection mode in the next 10 minutes; 2) If a load is switched more than 5 times within the time range threshold, it will be mandatorily kept in grid-connection in the next 10 minutes. The thresholds (such as 5 times or 10 minutes) can be adjusted according to the situation of system operation.

IV. CASE STUDIES

Case studies on a commercial house are presented. The office rooms are equipped with a PV module, an ES unit, air conditioning, fluorescent lamps, desktop computers, and house appliances like electric kettle and coffee machine. The PV, ES and appliances are connected through the energy router, as shown in Fig. 1.

Fig. 7 shows the normal PV generation and total load profile of the office in a whole day. Simulation parameters are shown in Table 4.

It is assumed that utility grid failure occurs at 0 hour and power restores at t_1, as is shown in Fig.7. The PV module starts to work from t_2, so the prosumer enters parallel operation mode. Some loads are chosen by the matching
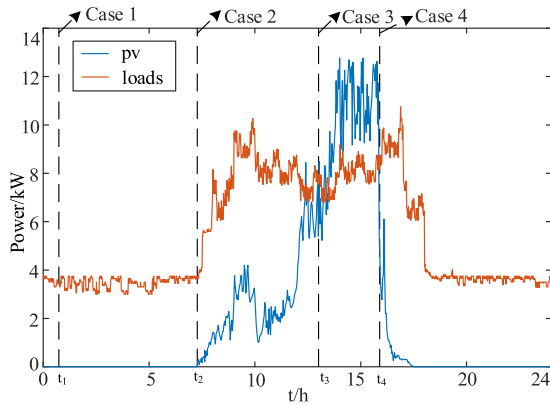
FIGURE 7. PV generation and load curves of an office room in a day.

algorithm to be powered by PV, while others are connected to the 1st AC bus and powered by the utility grid. After t_3, PV generation reaches above load demands, then the prosumer enters islanded mode. After t_4, PV power is lower than load demands, so the prosumer enters parallel mode from t_4. All the four cases of operation mode transition in Fig. 7 will be studied below.

A. CASE 1: ISLANDED MODE TO GRID-CONNECTED MODE

This case occurs at the early hour of the day when the PV unit has no power generation and the utility grid is recovering from a power failure. The prosumer is first powered by the ES unit (during 0-1s) and then transfers from islanded mode to grid-connected mode at 1s after grid supply restores. General loads are 2500W from 0-2s and 3500W from 2-3s.

The active and reactive powers of the two AC buses are shown in Fig. 8. As a result of power system fault between 0-1s, the loads are powered by ES unit in prosumer. Consequently, the active power of the 1st AC bus is 0 while the active power of the 2nd AC bus is 2500W. At 1s, the power grid restores from system fault. The active power of the 1st AC bus is negative because the current direction of the 2nd AC bus is defined positive.

B. CASE 2: GRID-CONNECTED MODE TO PARALLEL MODE

This case demonstrates the transition from grid-connected mode to parallel mode. Four loads are in operation in this case, their rated powers are 300W, 500W, 700W and 1000W respectively. The corresponding working time of 4 loads and power profiles of PV and total loads during 7:00 to 9:00 hour are shown in Fig. 9. As PV output is greater than the minimum load from 7:40h, the status of the prosumer during 7:00-7:40 is grid-connected mode and its status during 7:40-9:00 is parallel mode.

As shown in Fig. 9(b), the maximum utilization of PV power was achieved. Active power and reactive power of the 1st AC bus fluctuate at 7:30h when load3 is turned off. Load2 is switched to the 2nd AC bus through load matching at 7:42h. Load3 is then connected to the 2nd AC bus through
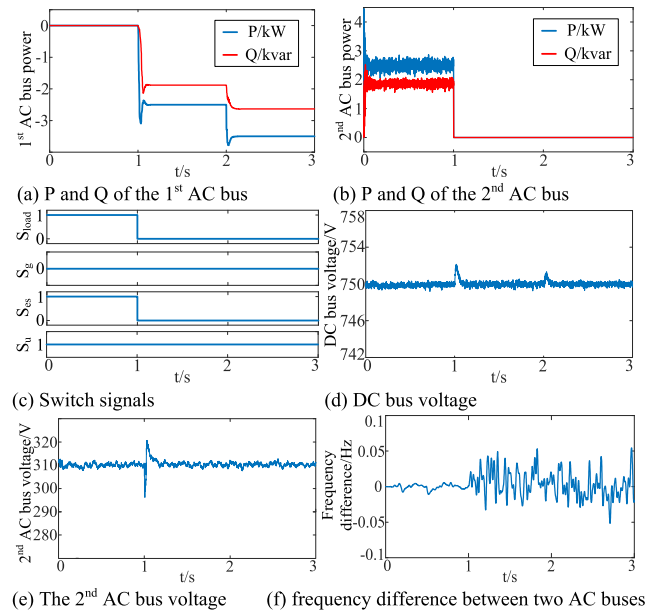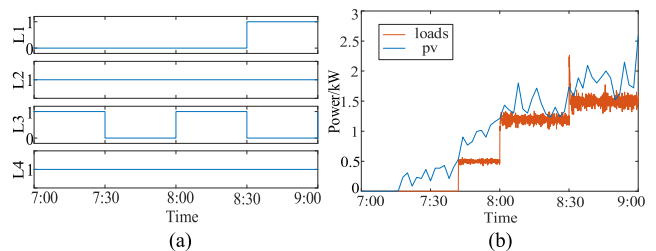

FIGURE 8. Profiles in case 1.

FIGURE 9. (a): Working hours of 4 loads; (b): PV and loads curves.

load matching at 8:00h as it starts to work again. Load4 is switched to the 2nd AC bus through load matching at 8:30. There are some glitches at 7:30, 7:42, 8:00 and 8:30 as loads changing. Simulation results are shown in Fig 10.

C. CASE 3: PARALLEL MODE TO ISLAND MODE

This case demonstrates the transition (at t_3) from parallel mode to islanded mode (from 12:00 to 14:00 hour). Seven loads (which are 1000W, 1000W, 1200W, 1300W, 1300W, 1300W and 420W respectively) as listed in Table 5 are in operation in this case. The corresponding working hours of these loads and power profiles of the PV and total loads are as shown in Fig. 11.

The prosumer system is in parallel mode from 12:00h to 13:42h, aiming for maximum utilization of the PV generation, and is in islanded mode from 13:42h to 14:00h. Active and reactive powers of the two AC buses are shown in Fig. 12(a) and (b). Although the power fluctuates at 12:12h, 12:42h and 13:12h because of load matching and switching, and then fluctuates at 13:42h as a result of transition from parallel mode to islanded mode, the power reaches new steady status in very short time, as shown in Fig. 12(a) and (b). The active and reactive powers on the 1st and 2nd AC buses are
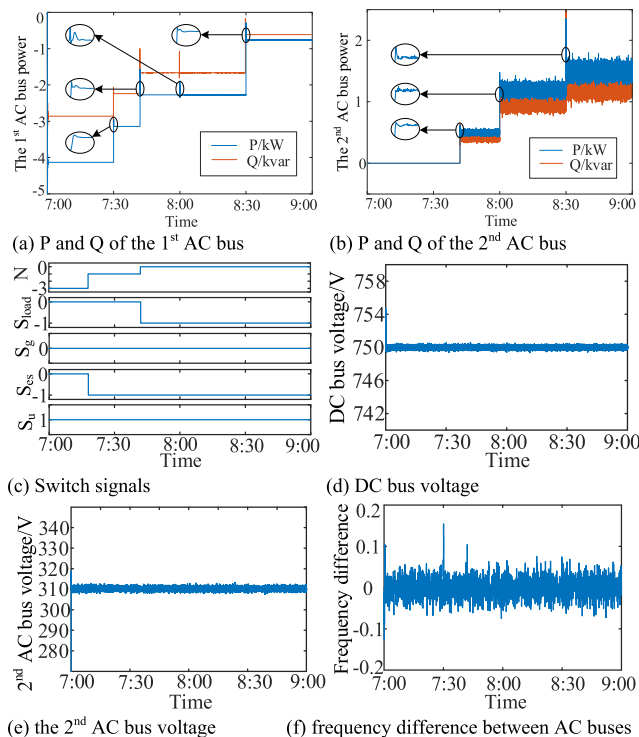
FIGURE 10. Profiles in case 2.

TABLE 5. Parameters of loads.

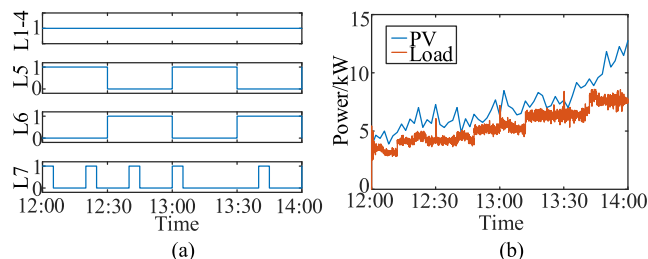|	P/W	Q/var
Load1	1000	750
Load2	1000	750
Load3	1200	900
Load4	1300	975
Load5	1300	975
Load6	1300	975
Load7	420	315

FIGURE 11. (a): Working hours of 4 loads; (b): PV and loads curves.

shown in Fig. 12(c)-(d). The DC and AC voltages are shown in Fig. 12(e)-(f).

FIGURE 12. Profiles in case 3.

FIGURE 13. Profiles in case 4.

D. CASE 4: ISLAND MODE TO PARALLEL MODE

This case demonstrates the transition from island mode to the parallel mode. There are five loads in operation, their power are rated as 7kW (group of electrical devices that do not require high power quality), 1kW, 1kW, 0.5kW and 0.5kW.
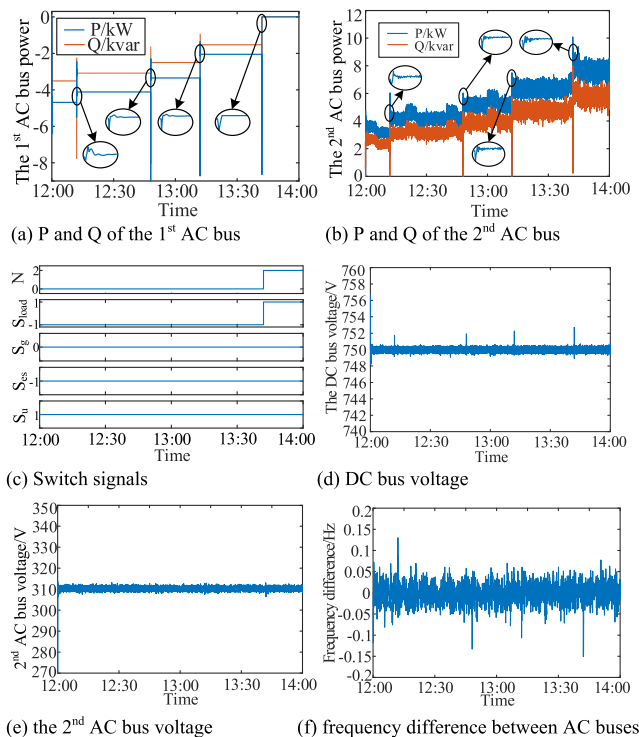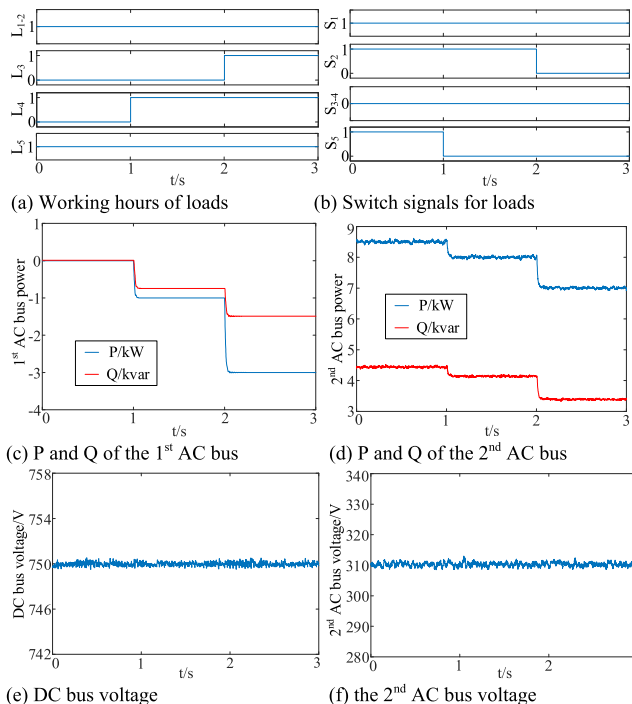
Their working hours are depicted in Fig. 13(a). In this case, the PV power output and total loads are shown in Fig. 13.

As can be seen, PV power output becomes lower than loads from 1s, so the prosumer will transfer to the parallel mode. Simulation results are shown in Fig. 13. Before 1s, the ES unit

is charging. Since the 2nd AC bus cannot support all the loads, some of them will be powered by utility grid. According to the power gap between the PV and the demands, the status of the switch array is updated so that load 2 and load 5 are switched from the 2nd to the 1st AC bus at 2s and 1s separately, as is shown in Fig. 13(b). The active and reactive powers on the 1st and 2nd AC buses are shown in Fig. 13(c)-(d). The DC and AC voltages are shown in Fig. 13(e)-(f).

V. CONCLUSION AND FUTURE WORK

This paper presents a novel energy router with multiple operation modes and elaborates on the analysis and its implementation in smart control and management for energy prosumers. Facilitated with the unique "parallel operation mode" and a fuzzy logic based hierarchical control strategy, the presented energy router is developed to enable full utilization of distributed renewable energies and flexible energy management, as well as maintain stable and reliable operation for the energy prosumer.

The transient power balance control in various operation modes for the energy prosumer has been investigated intensively. A hierarchical control strategy based on fuzzy controller is developed, and case studies on a commercial house are presented on the MATLAB/Simulink platform. Simulation results demonstrate that: 1) Full utilization of the DG generations can be achieved to reduce energy cost, while maintaining the transient stability of the prosumer by alleviating the negative effect of the DG fluctuations; 2) The switch array and parallel operation mode enable the loads to be optimally scheduled to keep pace with the DG generations, thus improve the system reliability and flexibly; 3) The hierarchical control strategy enables coordinated operation of the prosumer and seamless switching between the operation modes.

The presented energy router has the potential to enhance interconnections of energy prosumers in clusters and enable more friendly interactions with the utility grid. Therefore, our future work will focus on operation of prosumers in clusters where prosumers will have more interactions among each other and with the utility grid.

REFERENCES

[1] R. Abe, H. Taoka, and D. McQuilkin, "Digital grid: Communicative electrical grids of the future," *IEEE Trans. Smart Grid*, vol. 2, no. 2, pp. 399–410, Jun. 2011.

[2] C.-C. Lin, D.-J. Deng, C.-C. Kuo, and Y.-L. Liang, "Optimal charging control of energy storage and electric vehicle of an individual in the Internet of energy with energy trading," *IEEE Trans. Ind. Informat.*, vol. 14, no. 6, pp. 2570–2578, Jun. 2018.

[3] A. Zervos, C. Lins, and J. Muth, "RE-thinking 2050: A 100% renewable energy vision for the European Union," Eur. Renew. Energy Council, Brussels, Belgium, Tech. Rep., Apr. 2010.

[4] M. Z. Jacobson *et al.*, "100% clean and renewable wind, water, and sunlight all-sector energy roadmaps for 139 countries of the world," *Joule*, vol. 1, no. 1, pp. 108–121, Sep. 2017.

[5] L. Han, T. Morstyn, and M. McCulloch, "Incentivizing prosumer coalitions with energy management using cooperative game theory," *IEEE Trans. Power Syst.*, vol. 34, no. 1, pp. 303–313, Jan. 2019.

[6] J. Hu, Y. Li, and H. Zhou, "Energy management strategy for a society of prosumers under the IOT environment considering the network constraints," *IEEE Access*, vol. 7, pp. 57760–57768, 2019.

[7] R. A. Walling, R. Saint, R. C. Dugan, J. Burke, and L. A. Kojovic, "Summary of distributed resources impact on power delivery systems," *IEEE Trans. Power Del.*, vol. 23, no. 3, pp. 1636–1644, Jul. 2008.

[8] R. Tonkoski, D. Turcotte, and T. H. M. El-Fouly, "Impact of high PV penetration on voltage profiles in residential neighborhoods," *IEEE Trans. Sustain. Energy*, vol. 3, no. 3, pp. 518–527, Jul. 2012.

[9] I. Syed and V. Khadkikar, "Replacing the grid interface transformer in wind energy conversion system with solid-state transformer," *IEEE Trans. Power Syst.*, vol. 32, no. 3, pp. 2152–2160, May 2017.

[10] S. Madhusoodhanan, A. Tripathi, D. Patel, K. Mainali, A. Kadavelugu, S. Hazra, S. Bhattacharya, and K. Hatua, "Solid-state transformer and MV grid tie applications enabled by 15 kV SiC IGBTs and 10 kV SiC MOSFETs based multilevel converters," *IEEE Trans. Ind. Appl.*, vol. 51, no. 4, pp. 3343–3360, Jul. 2015.

[11] H. Qin and J. W. Kimball, "Solid-state transformer architecture using AC-AC dual-active-bridge converter," *IEEE Trans. Ind. Electron.*, vol. 60, no. 9, pp. 3720–3730, Sep. 2013.

[12] H. Guo, F. Wang, L. Zhang, and J. Luo, "A hierarchical optimization strategy of the energy router-based energy Internet," *IEEE Trans. Power Syst.*, vol. 34, no. 6, pp. 4177–4185, Nov. 2019.

[13] B. Liu, W. Wu, C. Zhou, C. Mao, D. Wang, Q. Duan, and G. Sha, "An AC–DC hybrid multi-port energy router with coordinated control and energy management strategies," *IEEE Access*, vol. 7, pp. 109069–109082, 2019.

[14] Y. Liu, Y. Fang, and J. Li, "Interconnecting microgrids via the energy router with smart energy management," *Energies*, vol. 10, no. 9, p. 1297, Aug. 2017.

[15] S. Parhizi, H. Lotfi, A. Khodaei, and S. Bahramirad, "State of the art in research on microgrids: A review," *IEEE Access*, vol. 3, pp. 890–925, 2015.

[16] B. Liu, J. Chen, Y. Zhu, Y. Liu, and Y. Shi, "Distributed control strategy of a microgrid community with an energy router," *IET Gener., Transmiss. Distrib.*, vol. 12, no. 17, pp. 4009–4015, Sep. 2018.

[17] D. Wang and F. Z. Peng, "Smart gateway grid: A DG-based residential electric power supply system," *IEEE Trans. Smart Grid*, vol. 3, no. 4, pp. 2232–2239, Dec. 2012.

[18] R. Takahashi, Y. Kitamori, and T. Hikihara, "AC power local network with multiple power routers," *Energies*, vol. 6, no. 12, pp. 6293–6303, Dec. 2013.

[19] R. Takahashi, K. Tashiro, and T. Hikihara, "Router for power packet distribution network: Design and experimental verification," *IEEE Trans. Smart Grid*, vol. 6, no. 2, pp. 618–626, Mar. 2015.

[20] P. Goncalves Da Silva, D. Ilic, and S. Karnouskos, "The impact of smart grid prosumer grouping on forecasting accuracy and its benefits for local electricity market trading," *IEEE Trans. Smart Grid*, vol. 5, no. 1, pp. 402–410, Jan. 2014.

[21] A. C. Luna, N. L. Diaz, M. Graells, J. C. Vasquez, and J. M. Guerrero, "Cooperative energy management for a cluster of households prosumers," *IEEE Trans. Consum. Electron.*, vol. 62, no. 3, pp. 235–242, Aug. 2016.

[22] Y. Cai, T. Huang, E. Bompard, Y. Cao, and Y. Li, "Self-sustainable community of electricity prosumers in the emerging distribution system," *IEEE Trans. Smart Grid*, vol. 8, no. 5, pp. 2207–2216, Sep. 2017.

[23] Q. Shafiee, T. Dragicevic, J. C. Vasquez, and J. M. Guerrero, "Hierarchical control for multiple DC-microgrids clusters," *IEEE Trans. Energy Convers.*, vol. 29, no. 4, pp. 922–933, Dec. 2014.

YINGSHU LIU was born in 1971. He received the B.S. and M.S. degrees from Zhejiang University, China, in 1993 and 1996, respectively, and the Ph. D. degree from Tianjin University, Tianjin, China, in 1999. He is currently an Associate Professor with the School of Electrical and Information Engineering, Tianjin University. His research interests include operation control strategy and energy management of microgrid, the energy Internet, energy router, and implementations of control and communication technologies in smart grid.

XI CHEN received the B.S. degree in electric engineering from the Huazhong University of Science and Technology, China, in 2016. He is currently pursuing the M.S. Degree at the School of Electrical and Information Engineering, Tianjin University, China. His research interest includes operation control strategy of microgrid and prosumer in power systems.

YAO WU received the B.S. degree in electric engineering from the Nanjing University of Science and Technology, China, in 2016, and the M.S. degree from the School of Electrical and Information Engineering, Tianjin University, China, in 2019. Her research interest includes operation control strategy and energy management of prosumers in smart grid.

KE YANG received the M.S. degree from the School of Electrical and Information Engineering, Tianjin University, China, in 2017. Her research interests include control strategy of energy storage unit and the ac/dc hybrid microgrid.

JIEBEI ZHU received the B.S. degree in microelectronics from Nankai University, Tianjin, China, in 2008, and the M.Sc. and Ph.D. degrees in electronic and electrical engineering from the University of Strathclyde, Glasgow, U.K., in 2009 and 2013, respectively. He is currently a Full Professor with the School of Electrical and Information Engineering, Tianjin University, supported by the 1000 Young Talents Program by the China Central Organization Committee. His research interests involve with HVdc transmission system control, renewable energy systems, and energy storage technologies. He was awarded with the license of Chartered Engineer by the U.K. Engineering Council and IET.

BIN LI received the B.Sc., M.Sc., and Ph.D. degrees in electrical engineering from Tianjin University, in 1999, 2002, and 2005, respectively. He completed his Postdoctoral research work at Tianjin University. In July 2006, he joined Tianjin University as an Associate Professor. From September 2006 to December 2006, he was ever an Academic Visitor with The University of Manchester, U.K. From September 2008 to September 2009, he worked in the design and application of protection relays and phasor measurement unit as a Bond Engineer at Areva Company, U.K. He is currently a Professor with the School of Electrical and Information Engineering, Tianjin University. He has published five books as a coauthor and more than 130 articles.

• • •